Journal of Inorganic Biochemistry 252 (2024) 112478

Contents lists available at ScienceDirect

Journal of Inorganic Biochemistry

journal homepage: www.elsevier.com/locate/jinorgbio

Zinc complexes of chloroquine and hydroxychloroquine versus the mixtures of their components: Structures, solution equilibria/speciation and cellular zinc uptake

Andrea Squarcina [a], Alicja Franke [a], Laura Senft [a], Constantin Onderka [b], Jens Langer [b], Thibaut Vignane [c], Milos R. Filipovic [c], Peter Grill [d], Bernhard Michalke [d], Ivana Ivanović-Burmazović [a,*]

[a] Department of Chemistry, Ludwig-Maximilians Universität (LMU) München, München 81377, Germany
[b] Department of Chemistry and Pharmacy, Friedrich-Alexander-Universität (FAU) Erlangen-Nürnberg, 91058 Erlangen, Germany
[c] Leibniz Institute for Analytical Sciences, ISAS e.V., 44227 Dortmund, Germany
[d] Research Unit Analytical BioGeoChemistry, Helmholtz Center Munich, 85764 Neuherberg, Germany

ARTICLE INFO

Keywords:
Zinc
Chloroquine
Ionophore
Solution equilibria
Zinc uptake

ABSTRACT

The zinc complexes of chloroquine (CQ; $[Zn(CQH^+)Cl_3]$) and hydroxychloroquine (HO-CQ; $[Zn(HO\text{-}CQH^+)Cl_3]$) were synthesized and characterized by X-Ray structure analysis, FT-IR, NMR, UV–Vis spectroscopy, and cryo-spray mass spectrometry in solid state as well as in aqueous and organic solvent solutions, respectively. In acetonitrile, up to two Zn^{2+} ions bind to CQ and HO-CQ through the tertiary amine and aromatic nitrogen atoms ($K^{CQ}_{N\text{-amin}} = (3.8 \pm 0.5)$ x $10^4\,M^{-1}$ and $K^{CQ}_{N\text{-arom}} = (9.0 \pm 0.7)$ x $10^3\,M^{-1}$ for CQ, and $K^{HO\text{-}CQ}_{N\text{-amin}} = (3.3 \pm 0.4)$ x $10^4\,M^{-1}$ and $K^{HO\text{-}CQ}_{N\text{-arom}} = (1.6 \pm 0.2)$ x $10^3\,M^{-1}$ for HO-CQ). In MOPS buffer (pH 7.4) the coordination proceeds through the partially deprotonated aromatic nitrogen, with the corresponding equilibrium constants of $K_{N\text{-arom}(aq)}{}^{CQ} = (3.9 \pm 1.9)$ x $10^3\,M^{-1}$ and $K^{HO\text{-}CQ}_{N\text{-arom}(aq)} = (0.7 + 0.4)$ x $10^3\,M^{-1}$ for CQ and HO-CQ, respectively. An apparent partition coefficient of 0.22 was found for $[Zn(CQH^+)Cl_3]$. Mouse embryonic fibroblast (MEF) cells were treated with pre-synthesized $[Zn((HO\text{-})CQH^+)Cl_3]$ complexes and corresponding $ZnCl_2$/(HO-)CQ mixtures and zinc uptake was determined by application of the fluorescence probe and ICP-OES measurements. Administration of pre-synthesized complexes led to higher total zinc levels than those obtained upon administration of the related zinc/(hydroxy)chloroquine mixtures. The differences in the zinc uptake between these two types of formulations were discussed in terms of different speciation and character of the complexes. The obtained results suggest that intact zinc complexes may exhibit biological effects distinct from that of the related zinc/ligand mixtures.

1. Introduction

Administration and cellular uptake of zinc, as the second most abundant bio-metal with a pivotal role in host immunity, have been related to numerous possible therapeutic applications, including treatments of malaria and coronavirus disease-2019 (COVID-19) [1,2]. In that line, the chemistry of zinc-drug interactions is of a particular interest [2d,f]. As one of the potential drugs to be used for the treatment of COVID-19, chloroquine (CQ) and its derivate hydroxychloroquine (HO-CQ) were initially discussed [2d]. In March 2020, the US Food and Drug Administration (FDA) issued an Emergency Use Authorization of HO-CQ and in many countries both CQ and HO-CQ were placed on the lists of treatment guidelines for COVID-19 [3]. Few months later, on June 15th 2020, FDA revoked the authorization for emergency use of CQ and HO-CQ, and the NIH recommended against their use for COVID-19, except in clinical trials [3c]. In fact, while a clinical study in China demonstrated that CQ treatment of COVID-19 patients had a clinical benefit versus control treatment and an open label non-randomized clinical trial with HO-CQ and azithromycin supported these findings, an international collaborative meta-analysis of randomized trials, published recently, showed no benefits and even increased mortality outcome in COVID-19 patients [4]. Independently from the controversy related to the anti-

* Corresponding author.
E-mail address: ivivch@cup.lmu.de (I. Ivanović-Burmazović).

https://doi.org/10.1016/j.jinorgbio.2024.112478
Received 26 October 2023; Received in revised form 22 December 2023; Accepted 2 January 2024
Available online 3 January 2024

SARS-CoV-2 activity of (hydroxy)chloroquine, they are in use to prevent and treat malaria, as well as autoimmune disorder such as rheumatoid arthritis and lupus [5]. Furthermore, zinc's ability to inhibit coronavirus replication were known even before COVID-19 pandemic started [6]. Several hypotheses were raised in the past year suggesting that improving zinc intake and/or combining it with (HO-)CQ (where (HO-)CQ = (hydroxy)chloroquine refers to both CQ and HO-CQ) could prove beneficial for COVID-19 patients [2f,7]. Another ongoing controversy is related to the effects of CQ and HO-CQ on cellular zinc uptake [8]. It has been reported that the combination of chloroquine with zinc increases Zn^{2+} uptake by A2780 cells and enhances chloroquine's anticancer activity [8a]. These results were questioned, because they were based on application of FluoZin-3 as a fluorescent sensor for intracellular zinc, which use demonstrated certain limitations (see section 3.6) [8b]. ICP-OES quantification of zinc in Madin–Darby canine kidney (MDCK) cells treated either with a combination of CQ and $ZnCl_2$ or with $ZnCl_2$ alone, resulted in the same intracellular zinc content, suggesting that chloroquine should not be considered as a zinc ionophore [8b]. The coordination of Zn^{2+} by HO-CQ was tested in ethanol and in aqueous, but zinc binding was not observed, although HO-CQ appeared to increase the zinc level in A549 cells (shown by using fluorescent stain FluoZin-3), which was attributed to a mechanism distinct from a ionophoric action of HO-CQ [8c].

To shed light on processes behind possible effects of (HO-)CQ on intracellular Zn^{2+} concentrations that are also relevant for designing and interpreting cell experiments, we were interested in solution properties of the Zn^{2+}-(hydroxy)chloroquine mixtures. Thus, we determined equilibrium constants for zinc binding to chloroquine and hydroxychloroquine, unknown in the literature, in both aqueous and organic medium that emulate the extracellular and membrane environment. Although binding of zinc to hydroxychloroquine was not observed in the literature [8c], using different experimental conditions (see below), besides quantification of corresponding binding constants, we could even synthesise and fully characterized the intact $[Zn(HO\text{-}CQH^{+})Cl_3]$ complex (i.e. **Zn(HO-CQ)**). In acetonitrile we could even observe binding of up to two Zn^{2+} to HO-CQ, as well as to CQ, whereas in buffer solutions at physiological pH = 7.4 both HO-CQ and CQ coordinate only one Zn^{2+}. Syntheses of $[Zn(CQ)Cl_2(H_2O)_2]$ and $[Zn(OAc)_2(CQ)(H_2O)]_2 \times H_2O$ were reported in the literature, however, the coordination mode of chloroquine and its complex structures were not experimentally confirmed [9]. In 2022, the first crystal structure of a Zn-chloroquine complex, $[Zn(CQH^{+})Cl_3]$ (**Zn(CQ)**), was deposited by us (CCDC 2081762). A year later, Paulikat et al. also reported the solid state structure of $[Zn(CQH^{+})Cl_3]$ determined by X-ray absorption and diffraction methods [10]. The authors characterized the binding mode of CQ in DMSO solution using NMR spectra of an equimolar CQ/$ZnCl_2$ mixture (and NMR spectra with $CoCl_2$, mimicking the Zn binding), the mass spectrum of the CQ/$ZnCl_2$ mixture and X-ray spectroscopy of a frozen DMSO solution [10]. They also simulated the Zn-CQ-water system by ab initio molecular dynamics [10]. The dynamic behaviour of Zn-(HO-)CQ complexes was theoretically approached by molecular dynamics and molecular docking, where it was shown that Zn(CQ/HO-CQ)$(Cl)_2(H_2O)$ complexes strongly bind and inhibit the main protease of COVID-19 (Mpro) [2f]. Here we provide further characterisation of the intact $[Zn(CQH^{+})Cl_3]$ complex (NMR, IR, UV–Vis and cryo-spray MS), including its stability constants in buffer and acetonitrile, as well as characterisation of its lipophilicity.

Using characterized pre-synthesized complexes $[Zn(CQH^{+})Cl_3]$ and $[Zn(HO\text{-}CQH^{+})Cl_3]$, we were able to compare their solution behaviour with that of the mixtures of their components (zinc and (HO-)CQ salts or their free base forms, respectively). Our goal was to probe, how possible differences in zinc solution speciation between two different complex formulations, pre-synthesized complexes (previously never been used in cell or other biological experiments) versus the mixtures of their components, may influence their zinc delivery efficiency into the cells. Interestingly, both **Zn(CQ)** and **Zn(HO-CQ)** complexes were more efficient in increasing the total intracellular levels of zinc than the mixtures of the corresponding components. Related to the enhanced zinc donating activity, these results suggest that defined complexes of Zn with CQ or HO-CQ, obtained in the neutral $[Zn(CQH^{+})Cl_3]$ or $[Zn(HO\text{-}CQH^{+})Cl_3]$ form, respectively, with kinetically less labile chloride ligands and of higher lipophilicity, could provide biological effects distinct from those of separate components or their mixtures, containing more labile, charged zinc aqua complexes of lower lipophilicity.

2. Materials and methods

Commercially available reagents were used directly, unless otherwise noted. Zinc chloride, triethylamine, diethyl ether, methanol, acetonitrile, dimethylsulfoxide, chloroquine diphosphate salt ($CQ\bullet H_3PO_4$), hydroxychloroquine sulfate ($HO\text{-}CQ\bullet H_2SO_4$), purchased by Sigma-Aldrich. Milli-Q water was used to prepare all the buffer solutions.

2.1. Synthetic procedures

$[Zn(CQH^{+})Cl_3]$ (Zn(CQ)). CQ (400 mg; 1.25 mmol) free base [11] was added to a solution of $ZnCl_2$ (150 mg; 1.10 mmol) in methanol (10 mL). The formation of a white precipitate was immediately observed. Methanol (10 mL) was added and the mixture was stirred at room temperature for 24 h. The white solid thus formed was filtered off, washed with methanol and subsequently with diethyl ether and dried under vacuum. Yield: 465 mg, 63%. Colourless crystals suitable for X-Ray analysis were obtained from an acetonitrile:methanol solution (1:1) by layering with ether at 4 °C.

UV–Vis (H_2O): λ_{max}/nm (ε/M^{-1} cm^{-1}) 256 ($1.5\bullet10^4$), 330 ($1.5\bullet10^4$), 343 ($1.5\bullet10^4$). **^{1}H NMR** (400 MHz, DMSO-d_6) δ [ppm] 0.95 (t, J = 6.6, 6H), 1.25 (d, J = 6.4, 3H), 1.55 (m, 3H), 1.67 (m, 1H), 2.50 (m, 6H), 3.81 (m, 1H), 6.69 (d, J = 6.1, 1H), 7.48 (d, J = 7.8 Hz, 1H), 7.54 (dd, J = 9.0, 2.2 Hz, 1H), 8.13 (s, 1H), 8.45 (m, 2H). **FT-IR** (ATR): ν (cm^{-1}) 3343(w), 3088(w), 2973(w), 2939(w), 2873(w), 2812(w), 1613(w), 1586(s), 1539(m), 1499(w), 1455(m), 1423(w), 1387(w), 1369(w), 1343(m), 1289(w), 1264(w), 1208(w), 1150(m), 1139(m), 1101(w), 1065(w), 948(w), 916(m), 863(s), 811(s), 760(m), 651(w), 614(w), 517 (m). **MS** (ESI) *m/z*) 454.0554 $[M\text{-}Cl]^+$, 490.0318 $[M+H]^+$. **Elemental Analysis**, calcd. For $C_{18}H_{27}Cl_4N_3Zn$: C = 43.89, H = 5.52, N = 8.53; found C = 44.48, H = 5.88, N = 8.25.

$[Zn(HO\text{-}CQH^{+})Cl_3]$ (Zn(HO-CQ)). Hydroxy-CQ (540 mg; 1.6 mmol) free base [11] was added to a solution of $ZnCl_2$ (200 mg; 1.6 mmol) in methanol (15 mL). The formation of a white precipitate was immediately observed. Methanol (15 mL) was added and the mixture was stirred at room temperature for 24 h. The white solid thus formed was filtered off, washed with methanol and subsequently with diethyl ether and dried under vacuum. Yield: 462 mg, 57%.

UV–Vis (H_2O): λ_{max}/nm (ε/M^{-1} cm^{-1}) 255 ($1.6\bullet10^4$), 330 ($1.3\bullet10^4$), 342 ($1.2\bullet10^4$). **^{1}H NMR** (400 MHz, DMSO-d_6) δ [ppm] 0.90 (t, J = 7.0, 3H), 1.24 (d, J = 6.3, 3H), 1.50 (m, 3H), 1.68 (m, 1H), 2.42(m, 6H), 3.38 (m, 2H), 3.79 (m, 1H), 4.27(s, 1H), 6.64 (d, J = 6.1, 1H), 7.37 (d, J = 7.5 Hz, 1H), 7.51 (dd, J = 9.0, 2.1 Hz, 1H), 8.05 (s, 1H), 8.42 (m, 2H). **FT-IR** (ATR): ν (cm^{-1}) 3343(w), 3020(w), 2976(w), 2936(w), 2872 (w), 1612(w), 1586(s), 1544(m), 1497(w), 1458(m), 1424(w), 1384(w), 1367(w), 1339(m), 1288(w), 1208(w), 1149(m), 1065(w), 949(w), 918 (w), 890(w), 858(s), 809(m), 760(m), 648(w), 614(w), 519(m). **MS** (ESI) *m/z*) 470.0498 $[M\text{-}Cl]^+$, 470.0503 $[M+H]^+$. **Elemental Analysis**, calcd. For $C_{18}H_{27}Cl_4N_3OZn$: C = 42.51, H = 5.35, N = 8.26; found C = 42.05, H = 5.39, N = 8.06.

2.2. General methods

FT-IR spectra were recorded Shimadzu ATR MIRacle 10 as solid samples from a diamond crystal. UV–Vis spectra were recorded with an Agilent Cary 60 UV-VIS-NIR spectrometer with a 10 mm quartz cuvettes.

NMR spectra were recorded with a Bruker AV400TR spectrometer. The spectrometers operated at 400 MHz for the proton nuclei. The chemical shifts of the NMR spectra are reported in ppm relative to the shift of the standard tetramethylsilane. ^{1}H NMR shifts are calibrated to the residual solvent resonances. In the report of the ^{1}H spectroscopic data, the multiplicity of the signals is abbreviated with s (singlet), d (doublet), t (triplet), and m (multiplet).

2.3. X-ray diffraction analysis

A colourless crystal of $[Zn(CQH^+)Cl_3]$ was embedded in inert perfluoropolyalkylether (viscosity 1800 cSt; ABCR GmbH) and mounted using a Hampton Research CryoLoop. The crystal was then flash cooled to 100.0(1) K in a nitrogen gas stream and kept at this temperature during the experiment. The crystal structure was measured on an Agilent SuperNova diffractometer with Atlas S2 detector using a CuKα microfocus source. The measured data was processed with the CrysAlisPro (v40.67a) software package [12]. Using Olex2, the structure was solved with the ShelXT structure solution program using Intrinsic Phasing and refined with the ShelXL refinement package using Least Squares Minimization [13–15]. All non-hydrogen atoms were refined anisotropically. Most hydrogen atoms were placed in ideal positions and refined as riding atoms with relative isotropic displacement parameters. The position of the hydrogen atoms at N2 and N3 were observed from difference Fourier maps and refined. The crystal structure data has been deposited with the Cambridge Crystallographic Data Centre. CCDC 2081762 contains the supplementary crystallographic data for complex $[Zn(CQH^+)Cl_3]$. This data can be obtained free of charge from The Cambridge Crystallographic Data Centre via www.ccdc.cam.ac.uk/data_request/cif. Crystallographic and refinement data is summarized in Table S1.

2.4. CSI-MS measurements

The CSI-MS experiments were performed on a UHR-TOF Bruker Daltonik maXis plus, an ESI-quadrupole time-of-flight (qToF) mass spectrometer capable of a resolution of at least 60.000 (FWHM), which was coupled to a Bruker Daltonik Cryospray unit. The measurements of solutions of pre-synthesized complexes or equimolar mixtures of $ZnCl_2$/(HO-)CQ (final concentrations $[Zn(CQ)] = [Zn(HO\text{-}CQ)] = 1 \times 10^{-5}$ M) in acetonitrile and water were performed in both positive and negative mode (the source voltage was 3.5 kV and the flow rate was 240 μL/h). Due to the poor solubility of neutral zinc complexes in aqueous medium, first they were dissolved in a small volume of organic solvent and then the resulting solution was diluted with water. The temperature of the spray gas (N_2) was held at −40 °C (5 °C for experiments in aqueous media) and the temperature of the dry gas for solvent removal was kept at −35 °C (5 °C for experiments in aqueous media). The mass spectrometer was calibrated prior to every experiment via direct infusion of Agilent ESI-TOF low concentration tuning mixture, which provided an *m/z* range of singly charged peaks up to 2700 Da in both ion modes. Applied solvents were not extra dry and could provide a source of protons. Processing of the measured data was done with Bruker Data Analysis 5.2.

2.5. UV-Vis titrations to determine the equilibrium constants for zinc-ligand complexation

Metal-ligand complexation titrations were performed in acetonitrile or in MOPS buffer (60 mM, pH 7.4) at 298 K by adding increasing volumes of acetonitrile solution of $ZnCl_2$ (0.01 M or 0.1 M) to the acetonitrile solution of chloroquine free base (CQ) or of hydroxychloroquine free base (HO-CQ). In the case of experiments performed in aqueous medium, buffered solutions of chloroquine diphosphate salt ($CQ\bullet 2H_3PO_4$) or hydroxychloroquine sulphate ($HO\text{-}CQ\bullet H_2SO_4$) were used. The metal-ligand complexation after addition of increasing concentration of $ZnCl_2$ titrant to the ligand solutions was followed by the absorbance change at the selected wavelength, (at 344 nm or 255 nm in acetonitrile or in MOPS, respectively). The equilibrium constants for the zinc-ligand complex formation, K, were calculated from the fit of experimental data (i.e. the dependence of absorbance at the selected wavelength vs $[Zn^{2+}]$) to Eq. (1) or (2) depending on the stoichiometry of the studied equilibria (i.e. binding of one or two Zn^{2+} ions to the one molecule of ligand, Eq. (1) or Eq. (2), respectively).

$$Abs = \left(A_0 + A_{end} \text{ x } K \text{ x } \left[Zn^{2+}\right]\right) / \left(1 + K \text{ x } \left[Zn^{2+}\right]\right) \quad (1)$$

$$Abs = \left(A_0 + A_1 \text{ x } K_1 \text{ x } \left[Zn^{2+}\right] + A_{end} \text{ x } K_1 \text{ x } K_2 \text{ x } \left[Zn^{2+}\right]^2\right) / \left(1 + K_1 \text{ x } \left[Zn^{2+}\right] + K_1 \text{ x } K_2 \text{ x } \left[Zn^{2+}\right]^2\right) \quad (2)$$

Where A_0, A_1 and A_{end} represent absorbance at the selected wavelength in the absence of Zn^{2+}, after binding of the first Zn^{2+} ion and for the fully formed metal-ligand complex, respectively, and $[Zn^{2+}]$ is the concentration of added $ZnCl_2$ in mol/l (M).

2.6. Partition coefficient determination

Distilled water-saturated 1-octanol and 1-octanol-saturated distilled water were obtained by extensive mixing of equal amounts of both solutions for 60 min, then separating and centrifuging each phase for 10 min at 1000 x g and discarding any residual minor phase [16]. For **Zn(CQ)**, the extinction coefficient (ε) at the local maxima at 344 nm was determined in 1-octanol saturated-distilled water by recording the absorbance of standard solutions and plotting of a corresponding calibration curve (Fig. S1). Due to the very low solubility of **Zn(HO-CQ)** in 1-octanol saturated-distilled water, that hindered the collection of a proper calibration curve, a partition coefficient for **Zn(HO-CQ)** could not be determined. The **Zn(CQ)** complexes was dissolved in a defined concentration in 1-octanol-saturated distilled water (3 mL) and mixed with equal volumes of distilled water-saturated 1-octanol. The two-phase mixture was shaken for 60 min at room temperature (300 rpm) on a plate shaker, the phases were separated via centrifugation (10 min, 25 °C, 1000 x g) and a UV/vis spectra of the aqueous phase were recorded. Under consideration of the determined extinction coefficient, the concentration of **Zn(CQ)** in each phase was calculated. The partition coefficient (log P) was determined using the equation:

$$log\ P = log\ \frac{[Zn(CQ)]octanol}{[Zn(CQ)]water}$$

2.7. Zinc uptake

Mouse embryonic fibroblast (MEF) cells were grown in Dulbecco's modified Eagle's media (DMEM, high glucose and sodium pyruvate, Gibco™, Cat#21969035) supplemented with 2 mM L-glutamine (Pan Biotech, Cat#P04–80100), 1% penicillin-streptomycin (Pan Biotech, Cat#P06–07100) and 10% Fetal bovine serum (Sigma Aldrich, Cat#F9665) at 37 °C and 5% CO_2. 80% confluent cells were incubated with 2 μM FluoZin-3 AM for 30 min. Cells were then washed and treated with 10 μM or 100 μM $ZnCl_2$, 100 μM CQ, 100 μM HO-CQ, 10 μM or 100 μM [Zn((HO)-CQ)] complexes, 100 μM chloroquine co-treated with either 10 μM or 100 μM $ZnCl_2$ or 100 μM hydroxy-chloroquine co-treated with 10 μM or 100 μM $ZnCl_2$ in PBS supplemented by 1 mg/mL glucose. In order not to interfere in the extracellular zinc speciation, no FBS was supplemented. Fluorescence of FluoZin-3 AM was recorded every 5 min for 4 h using CLARIOstarPlus (BMG labtech) microplate reader [17]. Excitation and emission wavelengths are 494 and 516 nm, respectively. Cell death was not observed during the four-hour treatments.

2.8. Zinc measurements by ICP-OES

80% confluent MEF cells were treated for one hour with 100 μM $ZnCl_2$, 100 μM CQ, 100 μM HO-CQ, 100 μM mixture of $ZnCl_2$ with either 100 μM of CQ or HO-CQ, as well as 100 μM **ZnCQ** or 100 μM **Zn(HO-CQ)**, respectively, in Earle's salt balanced media (Sigma Aldrich, Cat#E2888; no FBS was supplemented) [17]. Cells were washed 2 times with warm PBS, trypsinized and centrifuged at 300 xg for 5 min. Cell pellets were frozen and forwarded to the element analysis laboratory for further analysis. Cell pellets were transferred into closed quartz vessels and digested with HNO_3, suprapure, subboiling distilled (Merck, Darmstadt, Germany) in a microwave digestion system Discover® SP-D 80 (CEM corporation, Charlotte, North Carolina, USA). The resulting solution was filled up exactly to 10 mL with Milli-Q H_2O and was then ready for element determination. Zinc was determined employing an inductively coupled plasma optical emission spectrometer (ICP-OES) „ARCOS" (Spectro Ametek, Kleve, Germany), analysing the spectral element line at 213.856 nm. The sample introduction was carried out by a peristaltic pump, connected to a micromist nebulizer with a cyclon spray chamber. The RF power was set to 1400 W, the plasma gas was 15 L Ar /min, whereas the nebulizer gas was 0.6 L Ar/min. Regularly after ten measurements three blank determinations and a control determination of a certified standard (CPI) for all mentioned elements were performed. The results calculation was carried out on a computerized lab-data management system, relating the sample measurements to calibration curves, blank determinations and control standards.

3. Results and discussion

3.1. X-ray structure

The **Zn(CQ)** and **Zn(HO-CQ)** complexes have been obtained by mixing CQ and HO-CQ with zinc chloride in methanol at room temperature for 24 h (Scheme 1). Colourless crystals suitable for X-Ray analysis have been isolated for **Zn(CQ)** from an acetonitrile/methanol solution (1:1) by layering with ether at 4 °C.

The X-Ray analysis of **Zn(CQ)** shows a zwitterionic specie with a tetrahedral geometry for the metal center (Fig. 1, Table S1 in SI), in analogy to the very recently published structure obtained by synchrotron measurements and the one previously reported for a Zn-cinchonine complexes [10,18]. Due to a different synthetic procedure, the complex crystalizes in a P21/c space group, different from the Pbca space group recently reported [10]. In a related structure of L-histidinium trichlorozincate, (L-histidineH)-$ZnCl_3$, the histidine coordination occurs through the carboxylate group, instead of the more common histidine bidentate binding through two nitrogen atoms [19,20]. In zinc complexes the coordination geometry is mainly governed by the electrostatic repulsion between the electron pairs of the atoms bonded to the metal centre [21]. Thus in general, a tetrahedral arrangement of four ligands around the Zn center is the favourable geometry due to a lower repulsion between the coordinated species. The Zn^{2+} center in **Zn(CQ)** is coordinated by three chloride ions with a Zn—Cl bond length ranging between

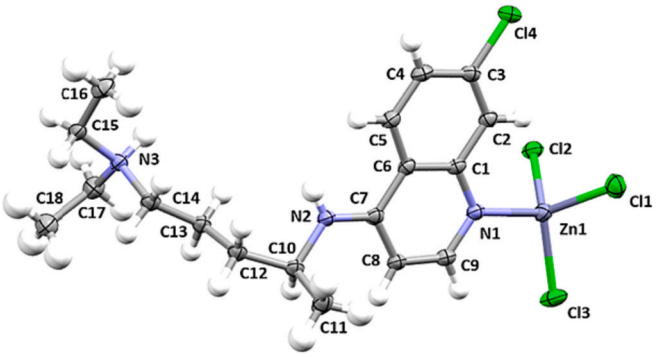

Fig. 1. Molecular structure of $[Zn(CQH^{+})Cl_3]$. Carbon atoms are depicted as grey ellipsoids, nitrogen atoms as blue ellipsoids, chlorine atoms as green ellipsoids and zinc atom as blue-grey ellipsoids. Thermal ellipsoids are shown at the 50% probability level. (For interpretation of the references to colour in this figure legend, the reader is referred to the web version of this article.)

2.241 and 2.291 Å (with the mean value of 2.270 Å), while binding of CQ through the aromatic N1 nitrogen of the quinoline ring with the Zn—N1 distance of 2.046 Å completes the coordination sphere (Fig. 1, Table S1). Just a negligible longer Zn—N1 bond length (2.051 Å) was recently reported for the same compound, whereas the mean value of Zn—Cl bond lengths was identical [10]. These values are comparable with those obtained for the Zn-cinchonine analogue, where again a longer Zn—N bond of 2.088 Å was observed (with the Zn—Cl distances in the 2.234–2.273 Å range) [18]. The zwitterionic specie is completed by the protonation of the tertiary amine N3 on the aliphatic tail of the CQ (Fig. 1). The X-Ray structures of the **Zn(CQ)** complex (firstly deposited by us and later reported by Paulikat et al.) represent the first structurally characterized CQ complex of a first row transition metal, thus being of biological relevance [10,22]. The only X-Ray structure previously reported for a metal complex with chloroquine was the one of PPh_3-Au(I)-CQ [22].

3.2. IR and NMR spectra

Coordination of the ligand through the quinoline moiety was also evident from the FT-ATR spectra of both **Zn(CQ)** and **Zn(HO-CQ)**, where the IR absorption bands characteristic for the quinoline "ring breathing" mode are shifted upon zinc binding and found at 1587–1542 cm^{-1} (Figs. S2 - S5) [23]. The perfect match between the IR spectra of **Zn(CQ)** and **Zn(HO-CQ)** in the fingerprint region (Fig. S6) suggests an analogue structure for the complexes and the same binding mode of the ligands. Furthermore, the Zn binding also causes a shift of the N—H stretching frequency of the secondary amine, for both complexes, from 3200 to 3344 cm^{-1} (Figs. S2 and S4). Due to the fact that the secondary amine group is in resonance with the quinoline aromatic system, it is affected by the coordination of the quinoline nitrogen to the Zn, as also evidenced by NMR (see below).

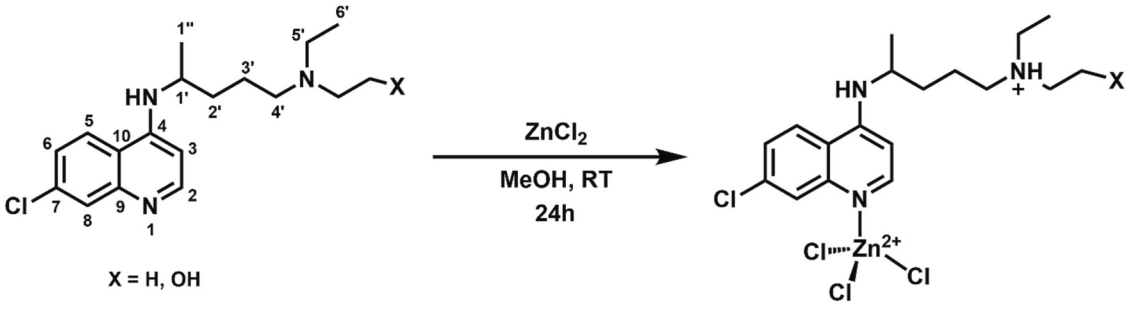

Scheme 1. Synthesis of the complexes, **Zn(CQ)** and **Zn(HO-CQ)**, and structural assembly from the crystal structure.

The comparison between the ^{1}H NMR spectra of the free ligands, CQ and HO-CQ, and their Zn complexes in d_6-DMSO provides additional information about the mode of zinc coordination in solution (Fig. S7 – S10). The difference between ^{1}H chemical shift for each NMR signal of the complex and the corresponding free ligand ($\Delta\delta$) can be used as a parameter to determine its binding mode in solution [10,24]. The biggest differences in the case of **Zn(CQ)** have been observed for the N—H proton of the secondary amine group ($\Delta\delta = 0.57$) and for the aromatic proton (H-8; $\Delta\delta = 0.37$) vicinal to N1 (Scheme 1 and Table 1). A similar shift for the H-8 ($\Delta\delta = 0.29$) and N—H ($\Delta\delta = 0.48$) protons have also been obtained for **Zn(HO-CQ)** (Table 2), again suggesting the same binding mode of CQ and HO-CQ in solution. Considering the solid-state structure of **Zn(CQ)**, with the ligand binding through the N1 atom, the shift observed for the N—H proton can be explained by the Zn coordination to quinoline nitrogen that influences the amino-imino tautomerism of the secondary amine group in resonance with the aromatic ring. The **Zn(CQ)** and **Zn(HO-CQ)** complexes were also generated in situ through the mixing of an equimolar concentration of $ZnCl_2$ with CQ or HO-CQ ligand in DMSO. The corresponding NMR spectra (Table S2 and S3 and Fig. S11-S12) suggest the same structure in DMSO solution for the species generated in situ as for the pre-synthesized complexes, although the observed H-8 and N—H shifts are significantly smaller than those for the pre-synthesized complexes. This behaviour is in agreement with a coordination equilibrium between Zn^{2+} and (HO-)CQ ligands (see below). While we measured the NMR spectra in aprotic DMSO, Paulikat et al. have recorded the NMR spectra of an equimolar CQ/$ZnCl_2$ mixture in the presence of a proton source ($DClO_4$) in DMSO [10]. However, they also observed a similar deshielding of H-8 and N—H signals upon Zn^{2+} addition at pD of 9.6. In addition, they reported a similar behaviour of the N—H signal, related to the tautomeric equilibria, in the NMR spectra of free CQ as a function of pD, further confirming our claims. Thus, the coordination of Zn, as a Lewis acid, and the protonation of the quinoline nitrogen have a similar impact on the electronic structure of CQ.

3.3. UHR-CSI mass spectra

The UHR-CSI mass spectra of both complexes were recorded in acetonitrile at −40 °C in order to detect the intact species present in solution and diminish the dissociation of the (HO-)CQ ligands. The species observed under such conditions in a positive ion mode are summarized in Table S4. The observed intact CQ complexes, $[(CQH^+)ZnCl_2]^+$ and $[(CQH_2^{2+})ZnCl_3]^+$ (Fig. S13), are probably generated by the Cl^- dissociation from or by the H^+ addition to the starting neutral complex, $[Zn(CQH^+)Cl_3]$, respectively. Similar molecular clusters were also observed by Paulikat et al. in DMSO solution of an equimolar CQ/$ZnCl_2$ mixture [10]. In the case of the zinc hydroxychloroquine complex two intact species were observed, $[(HO\text{-}CQ)ZnCl]^+$ and $[(HO\text{-}CQH^+)ZnCl_2]^+$ (Fig. S14), with the fully deprotonated and monoprotonated ligand forms, respectively. The absence of **Zn(CQ)** species with fully deprotonated CQ ligand under conditions of MS measurements (where residual protons are usually available in the ion source) is in agreement with the higher basicity of the tertiary amine in this ligand in comparison to that of HO-CQ.

In the MS spectra of the **Zn(CQ)** and **Zn(HO-CQ)** complexes in acetonitrile, the free CQ or HO-CQ ligands in their protonated $[(HO\text{-})CQH]^+$ and $[(HO\text{-})CQH_2]^{2+}$ forms were also detected (Table S4). This suggests the existence of an equilibria between the free ligands and zinc-chlorido species, in accordance with a labile nature of Zn complexes in solution (see below). The relative ratio of $[(HO\text{-})CQH]^+/[(HO\text{-})CQH_2]^{2+}$ peaks recorded for the **Zn(CQ)** and **Zn(HO-CQ)** complexes (Table S4) is also in agreement with a lower basicity of the tertiary amine of HO-CQ ligand in comparison to CQ. The measurements in negative ion mode confirmed the presence of the zinc trichlorido species, $[ZnCl_3]^-$, and thus the solution equilibria between the ligand free and the ligand bound Zn forms (vide infra). Such equilibria are usually solvent dependent. To prove that we also carried out the MS measurements in aqueous solution. No intact zinc complexes could be detected under such conditions, as expected due to an increased lability of Zn complexes in aqueous solution. The CSI-MS experiments performed in a positive mode for various mixtures of CQ or HO-CQ (free base) with zinc salts in acetonitrile at −40 °C, as well as in aqueous solution at 5 °C, did not confirm the existence of the intact **Zn(CQ)** or **Zn(HO-CQ)** complexes. Only mono- and di-protonated forms of the CQ or HO-CQ ligands could be detected under such conditions. This also suggests that the kinetics of the ligand coordination and dissociation, respectively, determine the speciation of the Zn complexes in solution (see below).

Table 1
^{1}H NMR in d_6-DMSO solution for **Zn(CQ)** and CQ (δ in ppm).

	2, 5	3	6	8	N-H	4′,5′	6′
Zn(CQ)	8.45	6.69	7.54	8.13	7.48	≈2.50	0.95
CQ	8.36	6.50	7.42	7.76	6.91	2.37	0.89
δ	0.09	0.19	0.12	0.37	0.57	0.13	0.06

Table 2
^{1}H NMR in d_6-DMSO solution for **Zn(HO-CQ)** and HO-CQ (δ in ppm).

	2, 5	3	6	8	N-H	4′,5′	6′
Zn(HO-CQ)	8.42	6.65	7.51	8.05	7.37	2.43	0.90
HO-CQ	8.36	6.49	7.42	7.76	6.89	2.43	0.90
δ	0.06	0.16	0.09	0.29	0.48	0.00	0.00

3.4. UV-Vis studies and determination of zinc binding equilibrium constants

The UV–Vis spectra of the CQ and HO-CQ ligands in acetonitrile display π-π* transitions in the 330–344 nm region characteristic for the aromatic system, as well as transitions in the far UV region (ca. 216–222 nm) that are related to the presence of the tertiary amine [25]. The UV–Vis spectrum of the CQ free base dissolved in acetonitrile indicates the presence of the species with a deprotonated aromatic nitrogen, as can be revealed from the existence of a single band at 330 nm [25]. Since the CQ ligand was dissolved in its free base form, it is reasonable to assume that in acetonitrile, as aprotic solvent, the tertiary amine group remains deprotonated, i.e. CQ exists as di-basic species under such conditions. This is confirmed by the results obtained from a titration of CQ with Zn^{2+} (Fig. 2). Namely, the addition of increased concentrations of Zn^{2+} (0–4.5 mM) to a 8 μM solution of CQ in acetonitrile leads to some spectral changes with an unclear isosbestic points in the UV region, indicating the occurrence of a biphasic binding of zinc cations, i.e. two subsequent Zn^{2+} binding equilibria (Fig. 2).

The initial spectral changes with isosbestic points at 223 and 258 nm are characterized by substantial absorbance decrease at 216 nm and somewhat smaller absorbance increase at 330 nm. It should be noted that the shape of the latter band remains unchanged, indicating that the Zn^{2+} binding to CQ in the first equilibrium is not related to the zinc binding to aromatic nitrogen, but to the deprotonated nitrogen of the tertiary amine. Although not previously observed, this behaviour is expected, since the basicity of the tertiary amine is about two units higher than that of the aromatic nitrogen [25]. A further increase of the zinc concentration in the acetonitrile solution of CQ leads to the subsequent spectral changes that are characterized by an increase in absorbance at 222, 237, 256 nm and by a substantial absorbance increase in the region of aromatic transitions, accompanied by the splitting into two bands at 330 nm and 344 nm (Fig. 2). The existence of the double peak in the aromatic region can be ascribed either to the existence of the aromatic nitrogen in its protonated form (seen, for example, in the neutral or acidic solution of chloroquine) or to the binding of cation to the deprotonated aromatic nitrogen [25a]. Thus, the biphasic interaction of the free base CQ with Zn^{2+}, as a Lewis acid, resembles that related to its protonation equilibria of the tertiary amine and aromatic quinoline

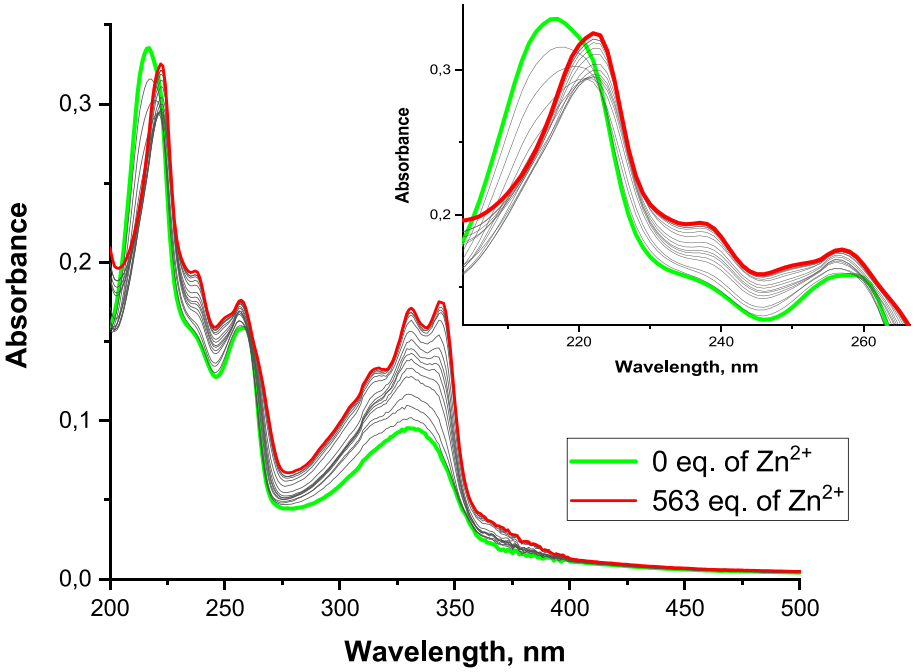

Fig. 2. Spectral changes recorded during titration of 8 μM solution of CQ (free base) with 0–4.5 mM solution of $ZnCl_2$ in acetonitrile at 298 K. Green line: spectrum recorded in the absence of Zn^{2+}, red line: spectrum recorded after the addition of 4.5 mM of Zn^{2+} solution. Inset: magnified spectral changes in the far UV region indicating the existence of biphasic binding of zinc cations. (For interpretation of the references to colour in this figure legend, the reader is referred to the web version of this article.)

nitrogen. Consequently, the obtained titration data can be used to calculate the equilibrium constants for the zinc binding to both nitrogen centres of CQ. With that goal, the absorbance changes at 344 nm were followed as a function of the Zn^{2+} concentration (Fig. 3) and the experimental data were fitted to the Eq. (2), describing the subsequent binding of two zinc cations to the CQ ligand with the equilibrium constants $K^{CQ}_{N\text{-}amin}$ and $K^{CQ}_{N\text{-}arom}$, for the zinc binding to the tertiary amine and aromatic nitrogen donor atoms, respectively (see Experimental Section for the detailed description of the fitting procedure). The fit of the experimental data with Eq. (2) results in $K^{CQ}_{N\text{-}amin} = (3.8 \pm 0.5) \times 10^4\ M^{-1}$

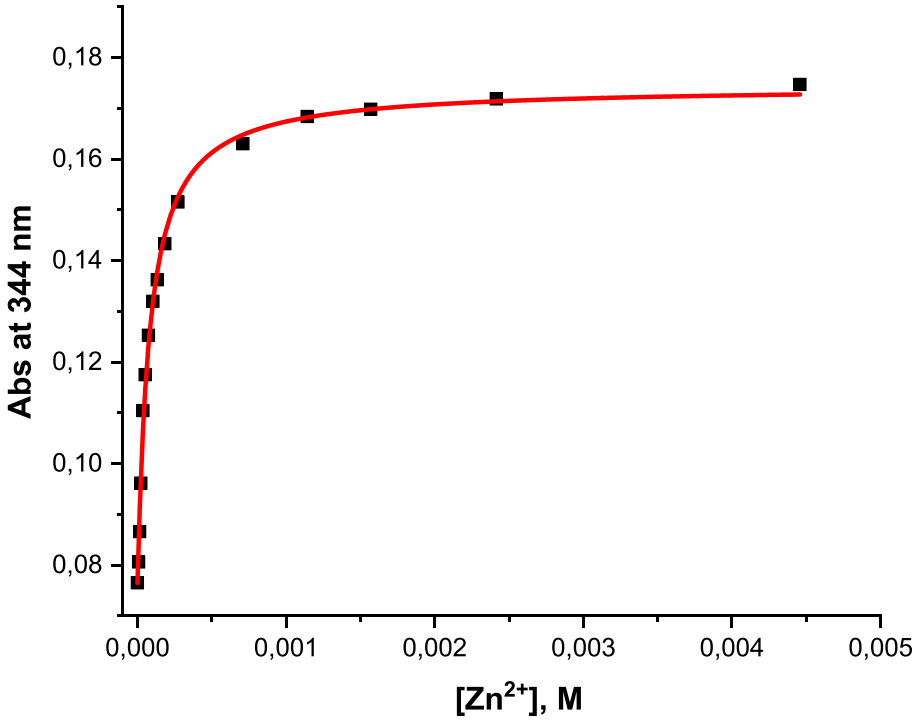

Fig. 3. Dependence of the absorbance at 344 nm, A_{344}, on $[Zn^{2+}]$ recorded for the biphasic zinc binding to free base CQ in acetonitrile. Experimental conditions: $[CQ] = 0.8 \times 10^{-5}$ M, $[Zn^{2+}] = 0$–4.5 mM in acetonitrile at 298 K. Red line: the fit of the experimental date to Eq. (2) in order to calculate the values of $K^{CQ}_{N\text{-}amin}$ and $K_{N\text{-}arom}{}^{CQ}$. (For interpretation of the references to colour in this figure legend, the reader is referred to the web version of this article.)

and $K^{CQ}_{N\text{-}arom} = (9.0 \pm 0.7)$ x $10^3\,M^{-1}$in acetonitrile at 298 K, displaying ca. 4 -fold higher affinity of zinc to the nitrogen of the tertiary amine than to the nitrogen atom of the aromatic ring, being in agreement with relative basicity of these nitrogen donor atoms.

Similar zinc titration experiments were performed for HO-CQ (free base) in acetonitrile (Fig. S15 and S16), resulting in the values for $K^{HO\text{-}CQ}_{N\text{-}amin} = (3.3 \pm 0.4)$ x $10^4\,M^{-1}$ and $K^{HO\text{-}CQ}_{N\text{-}arom} = (1.6 \pm 0.2)$ x $10^3\,M^{-1}$, being of the same order of magnitude as those determined for CQ. By way of comparison, in literature the zinc binding to tertiary amine moieties of α- and β-cyclodextrins could be observed in aqueous solution due to a lower basicity of their tertiary amine functionalities in comparison to those in (HO-)CQ (see below), resulting in the lower zinc binding constants ($K_{N\text{-}amin} = 5759 \pm 248$ and $K_{N\text{-}amin} = 9265 \pm 764\,M^{-1}$ for the functionalized α- and β-cyclodextrin, respectively) [26]. Importantly, the zinc binding to HO-CQ in ethanol was not observed in the literature, because instead of the free based, hydroxychloroquine sulfate (HO-CQ•H_2SO_4) was used [8c], which in non-aqueous solutions exists in a doubly protonated form that cannot coordinate metal centres. In addition, only up to 20 M excess of zinc over HO-CQ•H_2SO_4 was used, being significantly different from 530 M excess of zinc we applied (Fig. S15 and S16) [8c].

We also performed the zinc-ligand complexation titrations in buffered aqueous solution at pH = 7.4 (0.06 M MOPS). According to the literature, chloroquine ligand exhibits three protonation/deprotonation equilibria at $pK^{CQ}_{a1} \sim 4$, $pK^{CQ}_{a2} = 8.38$ and $pK^{CQ}_{a3} = 10.18$ that can be ascribed to the protonation/deprotonation events at the secondary amine, aromatic amidinium ion and tertiary amine, respectively [27]. Corresponding values found for hydroxychloroquine are: $pK^{HO\text{-}CQ}_{a1} < 4$, $pK^{HO\text{-}CQ}_{a2} = 8.27$ and $pK^{HO\text{-}CQ}_{a3} = 9.67$ [27]. The values of pK_{a1} and pK_{a2} for both ligands are similar, whereas the deprotonation of the tertiary amines in the case of HO-CQ proceeds at ca. 0.5 unit lower pH than for CQ ($pK^{HO\text{-}CQ}_{a3} = 9.67$ vs $pK^{CQ}_{a3} = 10.18$). This can be attributed to the formation of a hydrogen bond between the terminal OH and the tertiary amine of the side chain resulting in its lower basicity. A similar drop in pK_a values was observed going from triethylamine ($pK_a = 10.74$) to 2-diethylamino ethanol ($pK_a = 9.7$) [28].

Taking into consideration the reported pK_a values for both ligands it can be revealed that under physiological conditions (pH = 7.4), CQ and HO-CQ exist mainly as di-protonated species (protonated aromatic amidinium ion and a tertiary amine ($[(HO\text{-})CQH_2]^{2+}$) with a smaller fraction of monoprotonated species $[(HO\text{-})CQH]^+$ (ca. 10% or 11% of the total CQ or HO-CQ, respectively, with the deprotonated aromatic amidinium and secondary amine nitrogen). No Zn^{2+} binding to CQ or HO-CQ ligand was observed under pH = 5 or pH = 6.2 (data not shown), due to the protonation of the aromatic nitrogen. Contrary from a literature report where a lower zinc excess (up to 20 M equivalents of $ZnCl_2$) was used [8c], the presence of a small fraction of $[(HO\text{-})CQH]^+$ with deprotonated aromatic amine at pH = 7.4 enables the zinc binding, which shifts the coordination equilibrium between zinc ion and CQ or HO-CQ, respectively, towards complex formation (Fig. S17). Again, a significantly higher zinc excess over CQ and HO-CQ (up to 130 and 556 M equivalents of $ZnCl_2$, respectively) than the one used in the literature (see above) was required, in order to observe and quantify the zinc binding. The experimental data for the titration of CQ and HO-CQ in buffered aqueous solution at pH =7.4 were used to calculate the equilibrium constant for the binding of zinc ions to the aromatic nitrogen donor of CQ or HO-CQ (K^{CQ}_{aq} and $K^{HO\text{-}CQ}_{aq}$). The fit of the titration data to Eq. (1) (Fig. S17, see Material and Methods for a detailed description of the fit procedure) results in $K^{CQ}_{N\text{-}arom(aq)} = (3.9 \pm 1.9)$ x $10^3\,M^{-1}$and $K_{N\text{-}arom(aq)}{}^{HO\text{-}CQ} = (0.7 + 0.4)$ x $10^3\,M^{-1}$ in 0.06 mM MOPS, pH = 7.4, at 298 K. These values are lower than the corresponding values of equilibrium constants $K_{N\text{-}arom}$ determined for the free base ligands in acetonitrile under similar reaction conditions (Fig. 3 and Fig. S16). It should be noted that the results obtained in the buffered aqueous solutions are subjected to much larger experimental errors than in acetonitrile due to the limited solubility of the Zn^{2+} species at pH = 7.4 (i.e. with ongoing higher Zn^{2+} concentrations precipitation occurs). However, a lower stability of the zinc complexes with the monodentate bonded ligands in aqueous solution is expected and related to the more thermodynamically favoured formation of various zinc aqua species compared to that of other solvent species.

For further comparisons we summarize the zinc binding constants for selected mono- and polydentate ligands that are either structurally related to (HO-)CQ or of biological relevance (Table S5). The zinc binding ability of (HO-)CQ is similar to that of other monodentate ligands listed in Table S5 and is also comparable to that of histidylhistidine and glutamate, the latter existing in cells in concentrations of up to 100 mM. A significantly stronger binding is observed for bidentate and tridentate ligands with at least one negatively charged donor atom (Table S5).

It should be mentioned that the equilibria describing the zinc complexation to (hydroxy)chloroquine ligands in the titration experiments carried out in acetonitrile and in buffered aqueous solution differ from each other. The coordination of the chloroquine ligands to the zinc center will involve the substitution of coordinated water in $[Zn(H_2O)_x]^{2+}$ (being the predominant species at pH = 7.4; x = 4 or 6 for tetrahedral and octahedral aqua zinc complexes, respectively) and $[Zn(OH)(H_2O)_{x\text{-}1}]^+$ (ca. 2% pH = 7.4; x = 4–6) by the nitrogen donor atom of the aromatic ring of a positively charged $[(HO\text{-})CQH]^+$. In contrast, the formation of zinc complexes in acetonitrile involves the substitution of a chloride anion in $[ZnCl_4]^{2-}$ or $[ZnCl_3]^-$ by the nitrogen atoms of a tertiary and aromatic amine of the neutral CQ or HO-CQ ligands. The coordination sphere of the zinc in **Zn(CQ)** and **Zn(HO-CQ)** complexes is also assumed to be different in these two solvents. Namely, the titration in acetonitrile most probably leads to the formation of neutral or negatively charged $[Zn((HO\text{-})CQ)(Cl)_x]^{2\text{-}x}$ or $[Zn_2((HO\text{-})CQ)(Cl)_x]^{4\text{-}x}$ complexes (the coordination of one Zn^{2+}, through the tertiary amine, or of two Zn^{2+} ions, through tertiary and aromatic nitrogen, under a 1:1 condition or under an excess of zinc ions, respectively), whereas the titration in buffered aqueous solution at pH = 7.4 most likely results in the formation of positively charged $[Zn((HO\text{-})CQH^+)(H_2O)_x]^{3+}$ complexes.

3.5. Complex lipophilicity

To possibly evaluate the lipophilic character of $[Zn(CQH^+)Cl_3]$ and its affinity to cross the cell membrane, we determined its partition coefficient, between 1-octanol saturated by distilled water and distilled water saturated by1-octanol (log*P*), applying a standard procedure (see Materials and Methods). The obtained log*P* value of 0.22, however, cannot be attributed to the intact $[Zn(CQH^+)Cl_3]$ complex. The determination of the partition coefficients requires a quite extensive shaking of the complex in the presence of aqueous phase for 60 min, a procedure that inevitably accelerates the aquation of the pre-synthesized $[Zn(CQH^+)Cl_3]$ and favours the formation of charged, much more hydrophilic aqua species (e.g. $[Zn((HO\text{-})CQH^+)(H_2O)_x]^{3+}$, $[Zn(H_2O)_x]^{2+}$ or $[ZnCl(H_2O)_{x\text{-}1}]^+$, see above). Therefore, the obtained log*P* value can be considered as an apparent partition coefficient at certain experimental conditions. It is not related to a defined complex but rather to an equilibrium mixture. Considering the intact complex, due to its zwitterionic nature, a lower lipophilicity is expected than for the CQ free base (log*P* = 5.06) [27]. Because of its partial protonation, lipophilicity of CQ at pH 7.4 also drops significantly, illustrated by a so-called distribution coefficient log*D* = 0.92 [27]. This value represents an apparent partition coefficient at certain pH and it is not dramatically higher than the one we obtained for an aqueous product mixture of $[Zn(CQH^+)Cl_3]$. In addition, the charged aqua species resulting from aquation of $[Zn(CQH^+)Cl_3]$ are expected to be much more hydrophilic. Thus, it is expected that their presence in solution will lower the value of an apparent partition coefficient. By way of comparison, the biologically relevant cyanocobalamin that also exists in a neutral zwitterionic form (Co(III) coordinated by CN^- and deprotonated corrin ring has overall charge +1,

whereas the nucleotide loop has one negatively charged phosphate moiety) has the partition coefficient of only 0.025, thus being of lower lipophilicity than the equilibrium mixture of $[Zn(CQH^{+})Cl_3]$ in aqueous solution [29]. Furthermore, the charged Mn-porphyrin based antioxidants, even with long pyridyl alkyl chains with six or eight carbon atoms, exhibit much higher hydrophilicity than our system ($\log P = -2.29$ for MnTnHex-2-PyP and $\log P = -0.77$ for MnTnOct-2-PyP, respectively) [30]. However, they still exhibit a remarkably high drug accumulation that exceeded the drug levels in the cell medium [31]. Therefore, with the observed apparent partition coefficient that is at least a order of magnitude higher than those of Mn-porphyrins, one could expect an even more prominent cellular uptake for the $[Zn(CQH^{+})Cl_3]$ fraction present in the extracellular medium (see below).

Due to a quite restricted solubility of $[Zn(HO\text{-}CQH^{+})Cl_3]$ in aqueous solution, it was not possible to obtain a reliable value of its log*P* (see Materials and Methods).

3.6. Zinc uptake in MEF cells mediated by its *Zn(CQ)* and *Zn(HO-CQ)* complexes

At first, we assessed the cellular intake of **Zn(CQ)** and **Zn(HO-CQ)** by using a Zn fluorophore, FluoZin-3 AM. Different from the literature results, where the presence of chloroquine in a cell medium enhanced zinc uptake by a human ovarian cancer cell line (A2780), we did not observe a difference in the kinetics of Zn uptake over four hours between MEF cells treated with $ZnCl_2$ and those with $ZnCl_2$/CQ or $ZnCl_2$/HO-CQ mixtures (1:1 and 1:10), respectively (Fig. S18) [8a]. We suppose that the different observations are related to the differences in the experimental setups, including different cell types and $ZnCl_2$/CQ ratios used. Xue et al. applied higher excess of CQ over $ZnCl_2$ and stopped the treatment after 30 min. This may suggest that a higher CQ excess might push the equilibrium towards Zn coordination and that small portions of the formed complex may enter faster into the cell, an effect that might occur during a shorter treatment. However, in our studies the uptake of pre-synthesized **Zn(CQ)** and **Zn(HO-CQ)** showed the same saturation curves of the fluorophore as $ZnCl_2$ and the $ZnCl_2$/CQ and $ZnCl_2$/HO-CQ mixtures (Supplementary Figs. S18). It seems that all these treatments (either with $ZnCl_2$, its (HO-)CQ mixtures or with the **Zn(HO-)CQ** complexes) induced a high increase of a labile Zn^{2+} level (responsive to FluoZin-3), high enough to achieve the saturation of the signal obtained in MEF cells (incubated with 2 μM FluoZin-3), making the differentiation not possible. The obtained results also suggest that FluoZin-3 response to an exchangeable intracellular Zn^{2+} in MEF cells is not affected by the presence of Zn/(HO-)CQ mixtures or the **Zn (HO-)CQ** complexes. This was expected due to the high zinc binding constant of FluoZin-3 (Table S5). Based on the newest comprehensive study on the interference in the FluoZin-3 fluorescence performance by small molecular weight ligands (SMWL) present in the cell, only a small fraction of exchangeable zinc can be captured by FluoZin-3: ca. 4% of exchangeable Zn^{2+} pool in the form of Zn(FluoZin-3) and ca. 12% in the form of ternary Zn(FluoZin-3)(SMWL) complexes [32]. This leads to a significant underestimation of exchangeable Zn^{2+} detected by FluoZin-3 [32]. Thus it is not surprising that variations in the higher exogenously induced Zn levels cannot be registered by the FluoZin-3 fluorescence signal, which detection capacity is probably exceeded under particular cell experiment conditions. We investigated the possible formation of ternary Zn(FluoZin-3)((HO-)CQ) complexes by cryo-MS measurements, however we could not detect any species with the related composition. By way of comparison, for glutamate, the most abundant free metabolite present in cells (100 mM), with the zinc binding affinity similar to that of (HO-)CQ (Table S5), formation of a ternary complex was also not observed in the literature [32,33].

It is known that the variable cellular uptake of FluoZin-3, widespread heterogeneity in its localization and its differential accumulation, causes inconsistencies in the estimated labile Zn^{2+} levels, even under resting conditions [34]. In general, all the intensity-based dyes are prone to such behaviour, whit the fluorescence response depending not only on the zinc level but also on the cell internalization, e.i. the amount of probe present in a cell, its distribution and accumulation in a cell or in an organelle [34]. Therefore, to better understand if the cellular zinc uptake is influenced by the presence of (HO-)CQ in the cell medium or by its **Zn(HO-)CQ** complexes, we determined the total intracellular zinc levels by ICP-OES quantification (Fig. 4). Treatment of the cells with either 100 μM CQ or HO-CQ, as a control, did not significantly affect the intracellular levels of Zn, which were 65 ± 5 ng/mg protein, corresponding to ca. 200 μM total zinc concentration, being in the expected range of ca. 0.1–0.25 mM for eukaryotic cells [32,35,36]. A 36% decrease of cellular zinc concentration upon exposure of MDCK cells with 300 μM CQ for 1 h was reported in the literature [8b]. Different observations may result from the use of different cell types and different concentrations of CQ. The treatment with 100 μM $ZnCl_2$ increased the intracellular levels to 2.7 ± 0.9 μg/mg protein. The mixture of 100 μM Zn^{2+} with CQ and HO-CQ increased the zinc levels to 3.8 ± 1.2 and 1.9 ± 0.9 μg/mg protein, demonstrating within the experimental error limits that CQ and HO-CQ do not influence zinc uptake into MEF cells. The mixing of $ZnCl_2$ with the CQ or HO-CQ salts should lead to a binding scenario similar to the one seen in the titration experiments in the aqueous solution at pH = 7.4. However, the titrations were carried out in the presence of a weakly coordinating MOPS buffer and in the absence of other complexing agents, such as biological and inorganic anions, amino acids or coordinating buffer components (e.g. hydrogen phosphate anions from PBS). The latter, being components of the cell medium, will affect the zinc complexation equilibria involving CQ or HO-CQ ligands. For example, the PBS buffer (~ 12 mM) present in the cell medium will bind ca. 75% ($K_{Zn\text{-}phosphate} = 251.2\ M^{-1}$ at pH = 7.4, 298 K) of the added zinc ions (0.1 mM) [37]. Thus, the fraction of the zinc ions available for the complexation with (hydroxo)chloroquine ligands will significantly decrease in the cell medium, depending on the relative ratios and the values of the equilibrium binding constants involving other above-mentioned complexing agents in the biological medium. In addition, the amount of available zinc aqua species that can undergo complexation with the (hydroxo)chloroquine ligands in the cell medium will be considerably affected by the activity of the membrane-localized transporter proteins that control import/export of zinc from/to the extracellular environment. Thus, in view of these facts the estimation of the fraction of zinc ions complexed by (hydroxo)chloroquine ligands in the extracellular medium during the cell treatments with the $ZnCl_2$/(HO-)CQ mixtures seems to be rather complex, despite of the known values for the equilibrium constants determined for the zinc binding to these

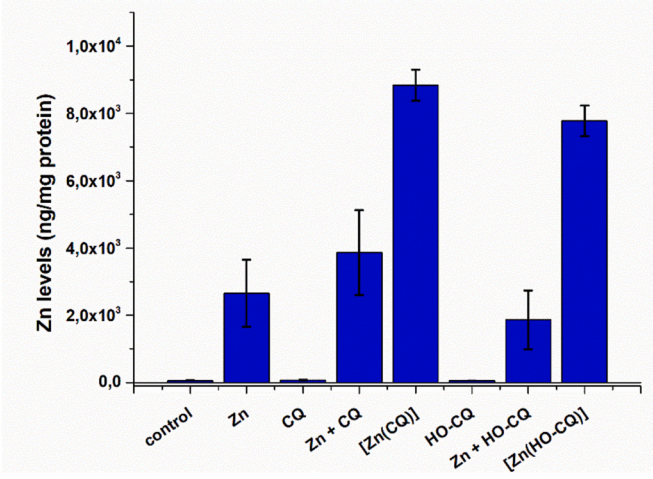

Fig. 4. Zinc levels in cells treated with **ZnCQ** or **Zn(HO-CQ)** complexes. Mouse embryonic fibroblasts were treated with 100 μM Zn^{2+}, its mixture with 100 μM CQ or HO-CQ, as well as with 100 μM **ZnCQ** and **Zn(HO-CQ)** complex and subjected to ICP-OES.

ligands in buffered aqueous solution. Similarly, it is difficult to state which fraction of the in situ generated $[Zn(CQH^+)(H_2O)_x]^{3+}$ complexes will cross the membrane to the intracellular environment during the cell incubation. Considering the positively charged nature of the aqua $[Zn(CQH^+)(H_2O)_x]^{3+}$ species, it can be supposed that their affinity to the lipophilic membrane should be rather low (see section 3.5). Therefore, it is not surprising that the treatment of MDCK cells with a CQ/$ZnCl_2$ mixture combined in a 6:1 ration (300 μM of CQ versus 50 μM $ZnCl_2$) also did not affected the intracellular zinc concentrations compared to the treatment with $ZnCl_2$ only [8b].

Besides thermodynamic considerations, the kinetic aspects are also relevant. The positively charged zinc aqua species $[Zn(H_2O)_x]^{2+}$ (x = 4 or 6) and $[ZnCl(H_2O)_{x-1}]^+$ (x = 4–6) with ca. 80% and 13% abundance, respectively, are the predominant species under conditions of up to 2 M chloride concentration [38] and of up to pH = 7.4 (e.g. a very small fraction of ca. 2% and 5% of $[Zn(OH)(H_2O)_{x-1}]^+$ (x = 4 or 6) exists at pH 7.4 and 7.8, respectively) [39]. Such aqua species are usually kinetically labile, whereas the neutral pre-synthesized $[Zn((HO-)CQH^+)Cl_3]$ complexes are rather kinetically inert towards ligand substitution [38]. The slower kinetics of chloride exchange are expected to undergo either an interchange dissociative (I_D) mechanism or to have a mixed character of an associative (A)/interchange associative (I_A) mechanism, compared to the faster dynamics of water exchanged on the zinc aqua species with a dissociative (D) type of the substitution mechanism [40].

All the above-mentioned considerations are in agreement with our finding, showing the total levels of zinc measured in the cells treated with either the pre-synthesized **ZnCQ** or **Zn(HO-CQ)** complex, being 8.8 ± 0.5 and 7.8 ± 0.5 μg/mg protein, respectively. These values are several-fold higher in comparison to those from the cells exposed to $ZnCl_2$ only or to the $ZnCl_2$/(HO-)CQ mixtures (Fig. 4). These results suggest that the neutral complexes $[Zn((HO-)CQH^+)Cl_3]$ can deliver a higher amounts of Zn into the cells than the simple mixtures of Zn and (hydroxy)chloroquine salts. The difference between the zinc levels in cells treated by **ZnCQ** or **Zn(HO-CQ)** are small. Although the stability constants of **Zn((HO-)CQ)** are not very high, they are higher than for phosphate and probably higher than for glutamine (estimated based on the values for glutamate; Table S5), as some of the major components of the used cell medium. As mentioned above, it seems more important that the kinetics of dissociation of the neutral $[Zn((HO-)CQH^+)Cl_3]$ complexes in aqueous (cell) medium are slower than their internalization into cells, enabling their uptake (Scheme 2). Based on the apparent partition coefficient of **ZnCQ,** significantly higher than those of Mn-porphyrins known to accumulate in cells to a remarkable extent [31], it is also assumed that the neutral $[Zn(CQH^+)Cl_3]$ fraction of the pre-synthesized complex present in solution will have a prominent tendency to cross the lipophilic membrane before it can undergo ligand substitution and equilibration reaction in the extracellular cell medium. Similarly, it is known from the literature that only neutral CQ or HO-CQ ligands can cross over the lipophilic membrane and reach the cellular cytosol, where they undergo protonation and increase the pH of the intracellular environment [41–45].

Whether these complexes are internalized into the cells in their intact forms is questionable. Certainly, their intracellular destiny is dependent on the thermodynamic and kinetic competition for zinc binding with several SMWL, peptides and surface protein functionalities. This depends on their zinc binding affinity, abundance, local pH conditions, as well as on the intracellular distribution/accumulation of these complexation agents and the internalized zinc species, respectively. For example, in certain intracellular compartments like lysosomes, it is expected that the $[Zn((HO-)CQH^+)Cl_3]$ complexes will undergo protonation at the aromatic nitrogen atom due to the lower pH found in such compartments in comparison to the pH of the extracellular medium. As a result, the zinc ions will be released and the CQ and HO-CQ ligands in their fully protonated form will accumulate inside the cells, being unable to cross over the membrane due to their positive charge.

Anyhow, it is evident that the Zn complexation by (HO-)CQ significantly enhances its accumulation in the cells and increases the fraction of labile zinc pool that can be buffered only by exchangeable zinc sites

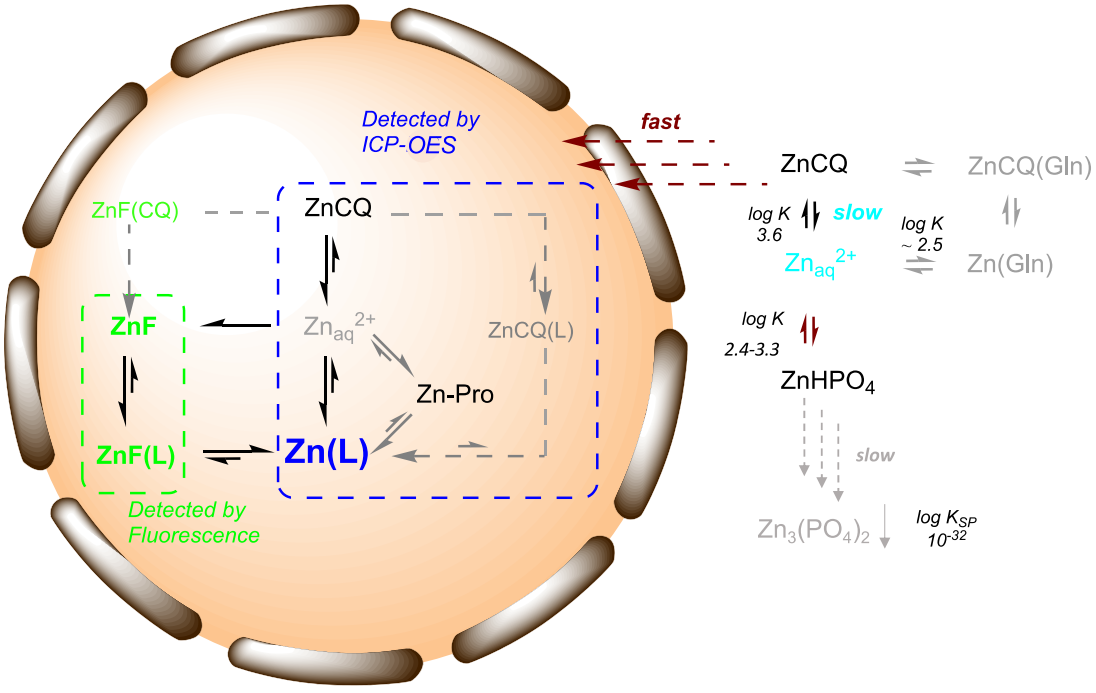

Scheme 2. Summary of the proposed processes operating in the extra- and intracellular environment as well as their interfaces during the cell treatments with the pre-synthesized **ZnCQ** complex, $ZnCl_2$ or the $ZnCl_2$/CQ mixtures. (For simplicity, free CQ forms, independent on their protonation state, are omitted from the equilibria with aqua Zn^{2+}_{aq} species). L refers to small molecular weight ligands (SMWL in the text); F = FluoZin-3; Gln = glutamine; Pro = protein surface binding sites). In light grey are represented the species that may be present in low amounts. A slow zinc phosphate precipitation can be expected based on the very low K_{sp} of $Zn_3(PO_4)_2$, but no precipitate was macroscopically observed during or after the cell incubation. Analogue processes are expected in the case of HO-CQ [32].

with sufficient binding capacity, e.g. predominantly by SMLW (L in Scheme 2) present in higher concentrations [32]. The prominent increase of the total intracellular zinc level we detected by ICP-OES in MEF cells treated with any of the extracellular zinc forms (either $ZnCl_2$, its mixtures with (HO-)CQ or their complexes), explains the saturation of FluoZin-3 fluorescence, whose binding capacity in an intracellular environment is significantly lower than the one of the endogenously present SMWL.

4. Conclusion

By determining the zinc binding equilibria with different protonated and basic forms of the ligands, as well as the speciation in the corresponding solutions of the pre-synthesized **Zn(HO-)CQ** complexes and the $ZnCl_2$/(HO-)CQ mixtures, respectively, we could shed light on the processes behind the increased zinc uptake in mouse embryonic fibroblast cells treated by the **Zn(HO-)CQ** complexes relative to that observed upon treatment with the $ZnCl_2$/(HO-)CQ mixtures. We could provide the evidence that a relatively weak complex may be biorelevant, if it is sufficiently inert to hydrolysis under physiologic conditions, being of general importance [46].

In solution, differently charged complexes with different lipophilicity, composition, thermodynamic stability and kinetic lability (such as $[Zn((HO\text{-})CQH^+)Cl_3]$, $[Zn(HO\text{-})CQ(Cl)_x]^{2-x}$, $[Zn_2(HO\text{-})CQ(Cl)_x]^{4-x}$ or $[Zn((HO\text{-})CQH^+)(H_2O)_x]^{3+}$) may exist in variable amounts. This depends on the solvent medium (e.g. its polarity), the coordination affinity of solvent molecules in comparison to the chloride, the mechanisms and the relative dynamics of their exchange (increases in the following order: $Cl^- <$ aqua $<$ acetonitrile). It also depends on the pH and the competition with other potential coordinating agents present in the extracellular medium in higher concentrations (such as phosphate). The interplay between factors determines the zinc speciation in the extracellular medium, which together with the mechanisms and ability of these species to cross the cell membrane determines the zinc influx. It seems that a neutral, rather lipophilic, character of the pre-synthesized (hydroxo)chloroquine $[Zn((HO\text{-})CQH^+)Cl_3]$ complexes and their relatively slow aquation and substitution with other potential ligands in the medium, respectively, favour the zinc uptake compared to the positively charged zinc aqua species $[Zn((HO\text{-})CQH^+)(H_2O)_x]^{3+}$, $[Zn(H_2O)_x]^{2+}$ or $[ZnCl(H_2O)_{x\text{-}1}]^+$ (main species in the solutions of extracellularly present $ZnCl_2$ and the $ZnCl_2$/(HO-)CQ mixtures; $x = 4$, 5 or 6). The latter are more prone to a faster water substitution and the consequent sequestration from the solution equilibria, e.g. in a form of $Zn_3(PO_4)_2$. A similar scenario is expected under true physiological conditions, where many other zinc coordinating agents (SMWL and proteins, e.g. albumin) are present. These agents may preferentially bind the more labile aqua, than chloro, species, resulting in a lower level of zinc internalized by the cells when the zinc aqua species are predominant in the extracellular surrounding [32,39,47,48].

Thus, the administration of the pre-synthesized complexes has a distinct effect on the zinc influx compared to the mixtures of Zn^{2+} with the corresponding ligands. In general, administration of defined zinc complexes with bio-active compounds as ligands, instead of corresponding mixtures, may be relevant to probe as a therapeutic approach. On this line, it would be interesting to compare in future studies the (pato)physiological consequences of these two forms (complexes vs. mixtures of their components) of zinc/(hydroxo)chloroquine administration.

CRediT authorship contribution statement

Andrea Squarcina: Formal analysis, Investigation, Methodology, Writing – original draft. **Alicja Franke:** Investigation, Writing - original draft. **Laura Senft:** Investigation. **Constantin Onderka:** Methodology. **Jens Langer:** Methodology. **Thibaut Vignane:** Data curation, Methodology. **Milos R. Filipovic:** Investigation, Methodology. **Peter Grill:** Data curation, Methodology. **Bernhard Michalke:** Data curation, Methodology, Validation. **Ivana Ivanović-Burmazović:** Conceptualization, Resources, Supervision, Validation, Writing – original draft, Writing – review & editing.

Declaration of competing interest

The authors declare no conflicts of interest.

Data availability

Data will be made available on request.

Acknowledgements

A.S., A.F., L.S. and I.I.-B. acknowledge support by Ludwig-Maximilians University München (LMU) and the Bayerisches Staatsministerium für Wissenschaft und Kunst.

Appendix A. Supplementary data

Supplementary data to this article can be found online at https://doi.org/10.1016/j.jinorgbio.2024.112478.

References

[1] E. Mocchegiani, M. Muzzioli, Therapeutic application of zinc in human immunodeficiency virus against opportunistic infections, J. Nutr. 130 (2000) 1424S–1431S.

[2] a) I. Wessels, B. Rolles, L. Rink, The potential impact of zinc supplementation on COVID-19 pathogenesis, Front. Immunol. 11 (2020) 1712;
b) A.V. Skalny, L. Rink, O.P. Ajsuvakova, M. Aschner, V.A. Gritsenko, S. Alekseenko, A.A. Svistunov, D. Petrakis, D.A. Spandidos, J. Aaseth, A. Tsatsakis, A.A. Tinkov, Zinc and respiratory tract infections: perspectives for COVID-19, Int. J. Mol. Med. 46 (2020) 17–26;
c) D. Jothimani, E. Kailasam, S. Danielraj, B. Nallathambi, H. Ramachandran, P. Sekar, S. Manoharan, V. Ramani, G. Narasimhan, I. Kaliamoorthy, M. Rela, COVID-19: poor outcomes in patients with zinc deficiency, Int. J. Infect. Dis. 100 (2020) 343–349;
d) M. Imran, W. Fatima, A.K. Alzahrani, N. Suhail, M.K. Alshammari, A. A. Alghitran, F.N. Alshammari, M.M. Ghoneim, S. Alshehri, F. Shakeel, Development of therapeutic and prophylactic zinc compositions for use against COVID-19: a glimpse of the trends, inventions, and patents, Nutrients 14 (2022) 1227–1243;
e) J. Veenemans, P. Milligan, A.M. Prentice, L.R.A. Schouten, N. Inja, A.C. van der Heijden, L.C.C. de Boer, E.J.S. Jansen, A.E. Koopmans, W.T.M. Enthoven, R. J. Kraaijenhagen, A.Y. Demir, D.R.A. Uges, E.V. Mbugi, H.F.J. Savelkoul, H. Verhoef, Effect of supplementation with zinc and other micronutrients on malaria in tanzanian children: a randomised trial, PLoS Med. 8 (2011) 1001125;
f) R.K. Hussein, H.M. Elkhair, Molecular docking identification for the efficacy of some zinc complexes with chloroquine and hydroxychloroquine against main protease of COVID-19, J. Mol. Struct. 1231 (2021) 129979.

[3] a) Office of the Commissioner, Emergency Use Authorization, U.S. Food and Drug Administration, 2020;
b) A. Dagens, L. Sigfrid, E. Cai, S. Lipworth, V. Cheng, E. Harris, P. Bannister, I. Rigby, P. Horby, Scope, quality, and inclusivity of clinical guidelines produced early in the covid-19 pandemic: rapid review, BMJ. 369 (2020) m1936;
c) A. Gasmi, M. Peana, S. Noor, R. Lysiuk, A. Menzel, A. Gasmi Benahmed, G. Bjørklund, Chloroquine and hydroxychloroquine in the treatment of COVID-19: the never-ending story, Appl. Microbiol. Biotechnol. 105 (2021) 1333–1343.

[4] a) J. Gao, Z. Tian, X. Yang, Breakthrough: chloroquine phosphate has shown apparent efficacy in treatment of COVID-19 associated pneumonia in clinical studies, Biosci. Trends 14 (2020) 72–73;
b) S. Arshad, P. Kilgore, Z.S. Chaudhry, G. Jacobsen, D.D. Wang, K. Huitsing, I. Brar, G.J. Alangaden, M.S. Ramesh, J.E. McKinnon, W. O'Neill, M. Zervos, H. Ford, COVID, Treatment with hydroxychloroquine, azithromycin, and combination in patients hospitalized with COVID-19, Int. J. Infect. Dis. 97 (2020) 396–403;
c) C. Axfors, A.M. Schmitt, P. Janiaud, J. Van't Hooft, S. Abd-Elsalam, E.F. Abdo, B.S. Abella, J. Akram, R.K. Amaravadi, D.C. Angus, Y.M. Arabi, S. Azhar, L. R. Baden, A.W. Baker, L. Belkhir, T. Benfield, M.A.H. Berrevoets, C.P. Chen, T. C. Chen, S.H. Cheng, C.Y. Cheng, W.S. Chung, Y.Z. Cohen, L.N. Cowan, O. Dalgard, F.F. de Almeida E. Val, M.V.G. de Lacerda, G.C. de Melo, L. Derde, V. Dubee, A. Elfakir, A.C. Gordon, C.M. Hernandez-Cardenas, T. Hills, A.I.M. Hoepelman, Y. W. Huang, B. Igau, R. Jin, F. Jurado-Camacho, K.S. Khan, P.G. Kremsner, B. Kreuels, C.Y. Kuo, T. Le, Y.C. Lin, W.P. Lin, T.H. Lin, M.N. Lyngbakken, C. McArthur, B.J. McVerry, P. Meza-Meneses, W.M. Monteiro, S.C. Morpeth, A. Mourad, M.J. Mulligan, S. Murthy, S. Naggie, S. Narayanasamy, A. Nichol, L.

A. Novack, S.M. O'Brien, N.L. Okeke, L. Perez, R. Perez-Padilla, L. Perrin, A. Remigio-Luna, N.E. Rivera-Martinez, F.W. Rockhold, S. Rodriguez-Llamazares, R. Rolfe, R. Rosa, H. Røsjø, V.S. Sampaio, T.B. Seto, M. Shahzad, S. Soliman, J. E. Stout, I. Thirion-Romero, A.B. Troxel, T.Y. Tseng, N.A. Turner, R.J. Ulrich, S. R. Walsh, S.A. Webb, J.M. Weehuizen, M. Velinova, H.L. Wong, R. Wrenn, F. G. Zampieri, W. Zhong, D. Moher, S.N. Goodman, J.P.A. Ioannidis, L.G. Hemkens, Mortality outcomes with hydroxychloroquine and chloroquine in COVID-19 from an international collaborative meta-analysis of randomized trials, Nat. Commun. 12 (2021) 2349.

[5] A. Kaul, C. Gordon, M.K. Crow, Z. Touma, M.B. Urowitz, R. van Vollenhoven, G. Ruiz-Irastorza, G. Hughes, Systemic lupus erythematosus, Nat. Rev. Dis. Primers 2 (2016) 16039.

[6] A.J.W. te Velthuis, S.H.E. van den Worm, A.C. Sims, R.S. Baric, E.J. Snijder, M. J. van Hemert, Zn2+ inhibits coronavirus and arterivirus RNA polymerase activity in vitro and zinc ionophores block the replication of these viruses in cell culture, PLoS Pathog. 6 (2010) e1001176.

[7] a) R. Derwand, M. Scholz, Does zinc supplementation enhance the clinical efficacy of chloroquine/hydroxychloroquine to win today's battle against COVID-19? Med. Hypotheses 142 (2020) 109815;
b) A. Pal, R. Squitti, M. Picozza, A. Pawar, M. Rongioletti, A.K. Dutta, S. Sahoo, K. Goswami, P. Sharma, R. Prasad, Zinc and COVID-19: basis of current clinical trials, Biol. Trace Elem. Res. 199 (2021) 2882–2892;
c) V. Cingolani, Hypothesis of zinc ascorbate as best zinc ionophore for raising antiviral resistance against Covid-19, J. Med. Virol. 93 (2021) 5205–5208;
d) A. Kumar, Y. Kubota, M. Chernov, H. Kasuya, Potential role of zinc supplementation in prophylaxis and treatment of COVID-19, Med. Hypotheses 144 (2020) 109848.

[8] a) J. Xue, A. Moyer, B. Peng, J. Wu, B.N. Hannafon, W.-Q. Ding, Chloroquine is a zinc ionophore, PLoS One 9 (2014) e109180;
b) J.P. Campos-Blázquez, N. Schuth, E. Garay, A.H. Clark, U. Vogelsang, M. Nachtegaal, R.G. Contreras, L. Quintanar, F. Missirlis, Chloroquine disrupts zinc storage granules in primary Malpighian tubule cells of Drosophila melanogaster, Metallomics 14 (2022) mfac075;
c) O.N. Kavanagh, S. Bhattacharya, L. Marchetti, R. Elmes, F. O'Sullivan, J. P. Farragher, S. Robinson, D. Thompson, G.M. Walker, Hydroxychloroquine does not function as a direct zinc Ionophore, Pharmaceutics 14 (2022) 899.

[9] M. Navarro, H. Goitia, P. Silva, M. Velásquez, L.E. Ojeda, G. Fraile, Synthesis and characterization of new copper– and zinc–chloroquine complexes and their activities on respiratory burst of polymorphonuclear leukocytes, J. Inorg. Biochem. 99 (2005) 1630–1636.

[10] M. Paulikat, D. Vitone, F.K. Schackert, N. Schuth, A. Barbanente, G. Piccini, E. Ippoliti, G. Rossetti, A.H. Clark, M. Nachtegaal, M. Haumann, H. Dau, P. Carloni, S. Geremia, R. De Zorzi, L. Quintanar, F. Arnesano, Molecular dynamics and structural studies of zinc chloroquine complexes, J. Chem. Inf. Model. 63 (2023) 161–172.

[11] R.A. Sanchez-Delgado, M. Navarro, H. Perez, J.A. Urbina, Toward a novel metal-based chemotherapy against tropical diseases. 2. Synthesis and antimalarial activity in vitro and in vivo of new ruthenium- and rhodium-chloroquine complexes, J. Med. Chem. 39 (1996) 1095–1099.

[12] Rigaku Oxford Diffraction, CrysAlisPro Software System, Version 1.171.40.67a, Rigaku Corporation, Oxford, UK, 2019.

[13] O.V. Dolomanov, L.J. Bourhis, R.J. Gildea, J.A.K. Howard, H. Puschmann, OLEX2 : a complete structure solution, refinement, J. Appl. Crystallogr. 42 (2009) 339–341.

[14] G.M. Sheldrick, SHELXT–integrated space-group and crystal-structure determination, Acta Cryst. A 71 (2015) 3–8.

[15] G.M. Sheldrick, Crystal structure refinement with SHELXL, Acta Cryst. C 71 (2015) 3–8.

[16] a) C.M. Weekley, I. Kenkel, R. Lippert, S. Wei, D. Lieb, T. Cranwell, J.L. Wedding, A.S. Zillmann, R. Rohr, M.R. Filipovic, I. Ivanović-Burmazović, H.H. Harris, Cellular fates of manganese(II) pentaazamacrocyclic superoxide dismutase (SOD) mimetics: fluorescently labeled MnSOD mimetics, X-ray absorption spectroscopy, and X-ray fluorescence microscopy studies, Inorg. Chem. 56 (2017) 6076–6093;
b) J.A. Arnott, S.L. Planey, The influence of lipophilicity in drug discovery and design, expert Opin, Drug Des. Discov. 7 (2012) 863–875.

[17] J.P.C. Coverdale, H.A. van den Berg, S. Khazaipoul, H.E. Bridgewater, A.J. Stewart, C.A. Blindauer, Albumin-mediated extracellular zinc speciation drives cellular zinc uptake, Chem. Commun. 58 (2022) 7384–7387.

[18] R. Hubel, K. Polborn, W. Beck, Metal complexes of biologically important ligands, cinchona alkaloids as versatile ambivalent ligands - coordination of transition metals to the four potential donor sites of quinine, Eur. J. Inorg. Chem. 471-482 (1999).

[19] M. Förster, R. Burth, A.K. Powell, T. Eiche, H. Vahrenkamp, Zinc complexes of amino acids and peptides, 2[1].- coordination of simple histidine derivatives to zinc, Chem. Ber. 126 (1993) 2643–2648.

[20] S.D. Dalosto, R. Calvo, J.L. Pizarro, M.I. Arriortua, Structure, disorder, and molecular dynamics in Zn(d,l-histidine)2: EPR of copper ion dopants, X-ray diffraction, and calorimetric studies, J. Phys. Chem. A 105 (2001) 1074–1085.

[21] I.L. Alberts, K. Nadassy, S.J. Wodak, Analysis of zinc binding sites in protein crystal structures, Protein Sci. 7 (1998) 1700–1716.

[22] a) M. Navarro, F. Vásquez, R.A. Sánchez-Delgado, H. Pérez, V. Sinou, J. Schrével, Toward a novel metal-based chemotherapy against tropical diseases. 7. Synthesis and in vitro antimalarial activity of new gold-chloroquine complexes, J. Med. Chem. 47 (2004) 5204–5209;
b M. Hitosugi-Levesque, J.M. Tanski, {4-[(7-Chloro-4-quinolyl)amino]-N,N-diethylpentanaminium}(triphenylphos-phine)gold(I) dinitrate, Acta Cryst E66 (2010) m1098–m1099.

[23] a) K. Nakamoto, Infrared and Raman Spectra of Inorganic and Coordination Compounds, 5th ed, New York, Wiley-Interscience, 1997;
b) A. Squarcina, D. Fehn, L. Senft, J. Langer, I. Ivanović-Burmazović, Dinuclear Zn complex: phenoxyl radical formation driven by superoxide coordination, Z. Anorg. Allg. Chem. 647 (2021) 809–814.

[24] J.Z. Dávalos, J. González, A. Guerrero, A.C. Valderrama-Negrón, L.D. Aguirre Méndez, R.M. Claramunt, D. Santa María, I. Alkortad, J. Elguero, A silver complex of chloroquine: synthesis, characterization and structural properties, New J. Chem. 37 (2013) 1391–1401.

[25] a) J.L. Irvin, E.M. Irvin, Spectrophotometric and potentiometric evaluation of apparent acid dissociation exponents of various 4-aminoquinolines, J. Am. Chem. Soc. 69 (1947) 1091–1099;
b) E. Tannenbaum, E.M. Coffin, A.J. Harrison, The far ultraviolet absorption spectra of simple alkyl amines, J. Chem. Phys. 21 (1953) 311–318.

[26] J. Warren, M. Bols, Zinc and copper complexes of methylated di- and tetraaminocyclodextrins, Eur. J. Org. Chem. 1083–1091 (2019).

[27] D.C. Warhurst, J.C.P. Steele, I.S. Adagu, J.C. Craig, C. Cullander, Hydroxychloroquine is much less active than chloroquine against chloroquine-resistant plasmodium falciparum, in agreement with its physicochemical properties, J. Antimicrob. Chemother. 52 (2003) 188–193.

[28] R.J. Little, M. Bos, G.J. Knoop, Dissociation constants of some alkanolamines at 293, 303, 318 and 333 K, J. Chem. Eng. Data 35 (1990) 276–277.

[29] M. Youssef, M. Ghorab, M. Khater, S. Gad, Effect of additives on intranasal preparation of cyanocobalamin, Int J Pharm Pharm Sci 7 (2015) 210–217.

[30] I. Kos, J.S. Rebouças, G. DeFreitas-Silva, D. Salvemini, Z. Vujaskovic, M. W. Dewhirst, I. Spasojević, I. Batinić-Haberle, Lipophilicity of potent porphyrin-based antioxidants: comparison of ortho and meta isomers of Mn(III) N-alkylpyridylporphyrins, Free Radic. Biol. Med. 47 (2009) 72–78.

[31] J.B. Aitken, E.L. Shearer, N.M. Giles, B. Lai, S. Vogt, J.S. Reboucas, I. Batinic-Haberle, P.A. Lay, G.I. Giles, Intracellular targeting and pharmacological activity of the superoxide dismutase mimics MnTE-2-PyP^{5+}and MnTnHex-2-PyP^{5+} regulated by their porphyrin ring substituents, Inorg. Chem. 52 (2013) 4121–4123.

[32] I. Marszałek, W. Goch, W. Bal, Ternary Zn(II) complexes of fluoZin-3 and the low molecular weight component of the exchangeable cellular zinc pool, Inorg. Chem. 57 (2018) 9826–9838.

[33] B.D. Bennett, E.H. Kimball, M. Gao, R. Osterhout, S.J. Van Dien, J.D. Rabinowitz, Absolute metabolite concentrations and implied enzyme active site occupancy in Escherichia coli, Nat. Chem. Biol. 5 (2009) 593–599.

[34] Y. Han, J.M. Goldberg, S.J. Lippard, A.E. Palmer, Superiority of SpiroZin2 versus FluoZin-3 for monitoring vesicular Zn^{2+} allows tracking of lysosomal Zn^{2+} pools, Sci. Rep. 8 (2018) 15034.

[35] M.R. Filipovic, J. Zivanovic, B. Alvarez, R. Banerjee, Chemical biology of H_2S signaling through Persulfidation, Chem. Rev. 118 (2018) 1253–1337.

[36] C.E. Outten, T.V. O'Halloran, Femtomolar sensitivity of metalloregulatory proteins controlling zinc homeostasis, Science 292 (2001) 2488–2492.

[37] D. Banerjea, T.A. Kaden, H. Sigel, Enhanced stability of ternary complexes in solution through the participation of heteroaromatic N bases. Comparison of the coordination tendency of pyridine, imidazole, ammonia, acetate, and hydrogen phosphate toward metal ion nitrilotriacetate complexes, Inorg. Chem. 20 (1981) 2586–2590.

[38] M.E. McMahon, R.J. Santucci Jr., J.R. Scully, Advanced chemical stability diagrams to predict the formation of complex zinc compounds in a chloride environment, RSC Adv. 9 (2019) 19905–19916.

[39] A. Krężel, W. Maret, The biological inorganic chemistry of zinc ions, Arch. Biochem. Biophys. 611 (2016) 3–19.

[40] N. Rampal, H.-W. Wang, D. Biriukov, A.B. Brady, J.C. Neuefeind, M. Předota, A. G. Stack, Local molecular environment drives speciation and reactivity of ion complexes in concentrated salt solution, J. Mol. Liq. 340 (2021) 116898.

[41] V. Ferrari, D.J. Cutler, Kinetics and thermodynamics of chloroquine and hydroxychloroquine transport across the human erythrocyte membrane, Biochem. Pharmacol. 41 (1991) 23–30.

[42] V. Ferrari, D.J. Cutler, Uptake of chloroquine by human erythrocytes, Biochem. Pharmacol. 39 (1990) 753–762.

[43] C. Rendal, K.O. Kusk, S. Trapp, The effect pf pH on the uptake and toxicity of the bivalent weak base chloroquine tested on Salix Viminalis and Daphnia Magna, Environ. Toxicol. Chem. 30 (2011) 354–359.

[44] Md. Mushtaque, Shahjahan, Reemergence of chloroquine (CQ) analogs as multi-targeting antimalarial agents: a review, Eur. J. Med. Chem. 90 (2015) 280–295.

[45] M. Chinappi, A. Via, P. Marcatili, A. Tramontano, On the mechanism of chloroquine resistance in plasmodium falciparum, PLoS One 5 (2010) e14064.

[46] This statement was made by one of reviewer.

[47] B. Petrovic, Ž.D. Bugarcić, A. Dees, I. Ivanovic-Burmazovic, F.W. Heinemann, R. Puchta, S.N. Steinmann, C. Corminboeuf, R. van Eldik, Role of π-acceptor effects in controlling the lability of novel monofunctional Pt(II) and Pd(II) complexes: crystal structure of [Pt(tripyridinedimethane)cl]cl, Inorg. Chem. 51 (2012) 1516–1529.

[48] M. Chrzanowska, A. Katafias, O. Impert, A. Kozakiewicz, A. Surdykowski, P. Brzozowska, A. Franke, A. Zahl, R. Puchta, R. van Eldik, Structure and reactivity of [RuII(terpy)(N^N)Cl]Cl complexes: consequences for biological applications, Dalton Trans. 46 (2017) 10264–10280.